ACS chemical biology

Articles

pubs.acs.org/acschemicalbiology

Selective Identification of Hedgehog Pathway Antagonists By Direct Analysis of Smoothened Ciliary Translocation

Yu Wang,[†,‡,∥,¶] Anthony C. Arvanites,[†,§] Lance Davidow,[†,§] Joel Blanchard,[†,§,#] Kelvin Lam,[†,§,□] Jin Woo Yoo,[⊥] Shannon Coy,[†,§,▽] Lee L. Rubin,*[,†,§] and Andrew P. McMahon*[,†,‡,§]

[†]Department of Stem Cell and Regenerative Biology, [‡]Department of Molecular and Cellular Biology, [§]Harvard Stem Cell Institute, [∥]Department of Chemistry and Chemical Biology, and [⊥]Harvard College, Harvard University, Cambridge, Massachusetts 02138, United States

Supporting Information

ABSTRACT: Hedgehog (Hh) signaling promotes tumorigenesis. The accumulation of the membrane protein Smoothened (Smo) within the primary cilium (PC) is a key event in Hh signal transduction, and many pharmacological inhibitors identified to date target Smo's actions. Smo ciliary translocation is inhibited by some pathway antagonists, while others promote ciliary accumulation, an outcome that can lead to a hypersensitive state on renewal of Hh signaling. To identify novel inhibitory compounds acting on the critical mechanistic transition of Smo accumulation, we established a high content screen to directly analyze Smo ciliary translocation. Screening thousands of compounds from annotated libraries of approved drugs and other agents, we identified several new classes of compounds that block Sonic hedgehog-driven Smo localization within the PC. Selective analysis was conducted on two classes of Smo antagonists. One of these, DY131, appears to inhibit Smo signaling through a common binding site shared by previously reported Smo agonists and antagonists. Antagonism by this class of compound is competed by high doses of Smo-binding agonists such as SAG and impaired by a mutation that generates a ligand-independent, oncogenic form of Smo (SmoM2). In contrast, a second antagonist of Smo accumulation within the PC, SMANT, was less sensitive to SAG-mediated competition and inhibited SmoM2 at concentrations similar to those that inhibit wild-type Smo. Our observations identify important differences among Hh antagonists and the potential for development of novel therapeutic approaches against mutant forms of Smo that are resistant to current therapeutic strategies.

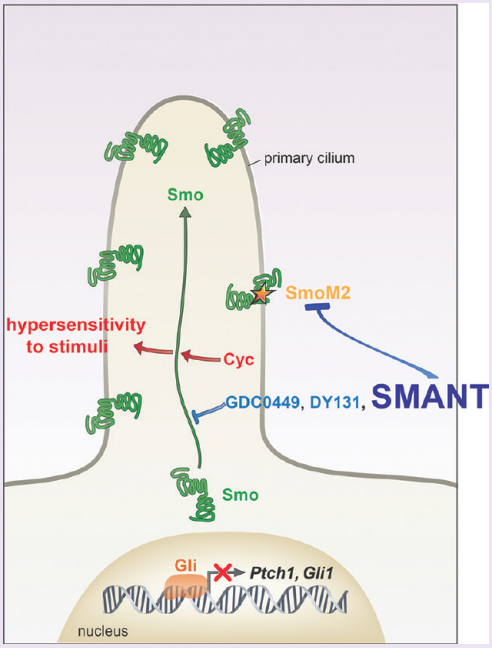

Hedgehog (Hh) signaling plays an essential role in developmental processes and adult tissue homeostasis.[1] An increasing body of evidence identifies the Hh pathway as a contributing factor in the growth of a variety of human cancers. The loss of normal regulatory control of the Hh pathway within a subset of Hh responsive cells leads directly to the initiation of particular solid tumors, notably basal cell carcinoma (BCC), the most prevalent cancer in the Caucasian population,[2] and medulloblastoma (MB), the most common childhood brain cancer.[3] In other cancers, Hh signals from tumor cells appear to condition the local environment to favor tumor growth. This category includes a broad spectrum of high incidence cancers, particularly those in the breast, lung, liver, stomach, pancreas, prostate, and gastrointestinal tract.[4] The potential of Hh targeted cancer therapy has stimulated an extensive search for Hh pathway antagonists. Typically, drug discovery screens have broadly sampled the Hh pathway looking for agents capable of silencing a Hh signal-dependent transcriptional response. Although small-molecule "hits" may occur at any point in the pathway that can ultimately translate into an altered transcriptional response, Smoothened (Smo) has emerged as the prevalent target.[5] Smo is essential for all pathway activity, and activating mutations in Smo have been observed in both human BCC and MB. Smo antagonists have entered clinical trials,[6] and successful repression of tumorigenesis in patients with invasive or metastatic forms of BCC has validated the concept of Hh targeted cancer therapy.[7] A leading drug, GDC0449 (now marketed as Erivedge), was recently approved by the U.S. Food and Drug Administration (FDA) for treatment of advanced BCC.[8]

An obligatory step in the activation of Hh signaling is the accumulation of Smo in the primary cilium (PC), a tubulin-scaffolded membrane extension templated by the centriole (Supplementary Figure 1).[9,10] While all small molecule Smo

Received: January 19, 2012
Accepted: March 28, 2012
Published: May 3, 2012

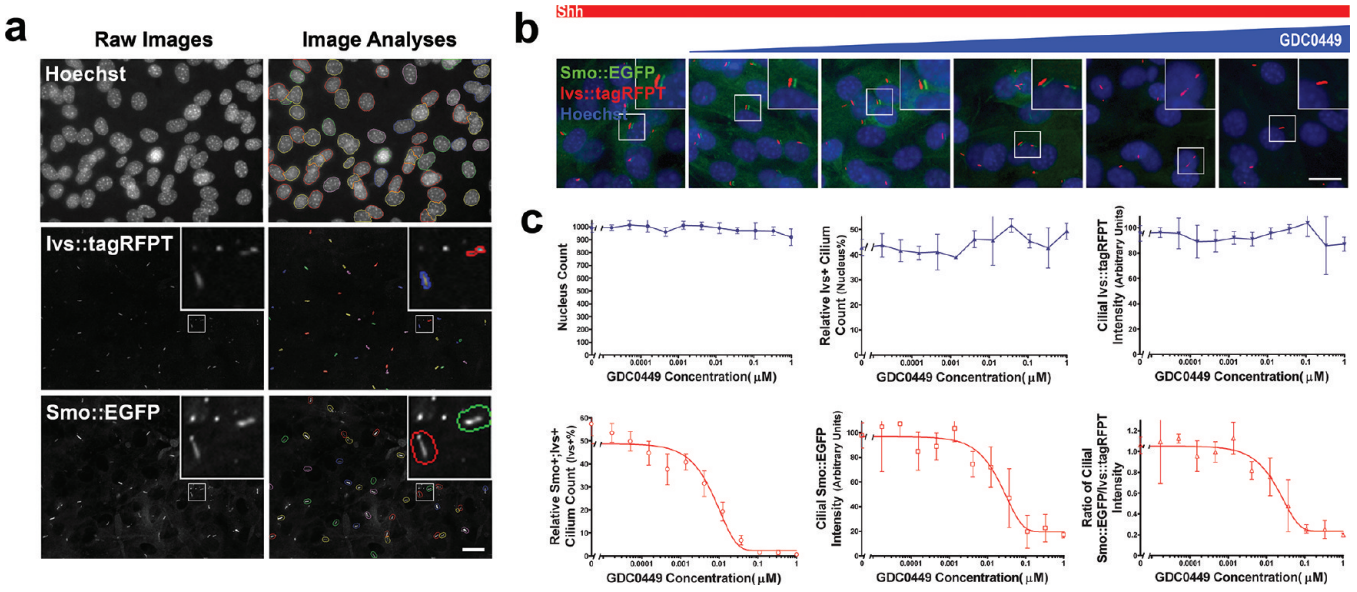

Figure 1. A high content Smo antagonist screen − image analysis and assay validation. (a) A field of cells in a typical well. The cell number was calculated by counting Hoechst stained nuclei. The PC were precisely segmented as Ivs::tagRFPT positive structures, and hSmo::EGFP intensity was quantified in the PC. (b) Representative images of the dose-dependent inhibition of Smo::EGFP ciliary accumulation by GDC0449. The concentrations of GDC0449 used to obtain these images were 0, 0.15 nM, 1.3 nM, 12 nM, 111 nM, and 1 μM from left to right. Scale bar: 10 μm. (c) Key measurements from high content image analyses. The cell number was determined by counting Hoechst stained nuclei. Ivs::tagRFPT positive structures were precisely segmented as the PC, and Smo::EGFP intensity within the PC was quantified. The Ivs+ cilium count and Smo+ cilium count were determined on the basis of arbitrary thresholds; the mean (±SD) shown is based on four replicates.

agonists examined so far induce Smo accumulation in the PC, various Smo antagonists affect Smo localization in distinct ways (Supplementary Figure 1).[11−13] SANT-1, SANT-2, and GDC0449 inhibit both Hh pathway activation and Sonic hedgehog (Shh) induced Smo accumulation within the PC.[11−13] In contrast, cyclopamine (cyc), a natural product from the plant *Veratrum californicum*, and its potent derivative KAAD-cyc bind Smo and inhibit pathway activation but behave as pseudoagonists promoting Smo accumulation within the PC.[11−14] Further, forskolin (FKL), a putative protein kinase A (PKA) activator, inhibits Hh pathway activity and indirectly promotes Smo ciliary accumulation through PKA stimulation.[11] Thus, there are distinct actions and outcomes associated with different inhibitory factors grouped around Smo action (Supplementary Figure 1).

To explore regulatory activity at this critical level of pathway action, we performed a direct screen for inhibitors of Smo translocation to the PC and identified 20 classes of inhibitory compounds. We identified some novel compounds that may act on Smo in a manner similar to that of previously identified antagonists and agonists, underscoring the chemical diversity of compound interactions at what is possibly a common site. However, we also identified a new compound, SMANT, that inhibits an oncogenic form of Smo refractory to inhibition by currently available Smo antagonists.

RESULTS AND DISCUSSION

Screening for Antagonists of Smo Translocation to the Primary Cilium. In work to be published elsewhere, we have established a high content screen for modulators of Smo translocation focusing on small molecules stimulating Smo translocation to the PC (Wang Y., et al., under revision). We then modified the system to identify inhibitors of Smo ciliary translocation. In brief, we developed a cell line producing human Smo::EGFP and Ivs::tagRFPT fusion proteins. Ivs::tagRFPT highlights the PC, and GFP enables the cellular trafficking of Smo to be visualized. Test compounds were added in low serum medium for 18−24 h in the presence of Shh, and cells were then fixed and stained with Hoechst (Supplementary Figure 2). Quantitative multiparametric image analyses were performed with custom algorithms (for details, please refer to Methods). The most critical parameters measured are indicated in Figure 1a: cell number was measured by counting Hoechst-labeled nuclei, whereas the PC was precisely segmented as an Ivs::tagRFPT positive structure. The specific PC localization of Smo::EGFP was discerned by applying a defined threshold for the length−width ratio of Ivs::tagRFPT positive structures (inset in Ivs::tagRFPT images) and then quantifying Smo::EGFP intensity within the Ivs::tagRFPT positive PC. Key measurements from these analyses are shown for GDC0449 (Figure 1b and c) and SANT-1 (Supplementary Figure 3). As expected, each specifically inhibited Smo::EGFP accumulation in the PC without causing significant structural changes to the PC itself or measurable cytotoxicity.[14−16]

We used this high content assay to screen a collection of approximately 5,600 small molecules for compounds that block Smo accumulation in the presence of Shh. The small molecule library includes FDA-approved drugs, drug candidates in preclinical or clinical development, and a group of compounds with annotated biological activity. Representative examples of assay plates are shown (Supplementary Figure 4). Z-prime scores[17] were consistently >0.6, confirming the robustness of the screen.

We first eliminated small molecules with "off-target" effects, *e.g.*, inhibitory effects on ciliary assembly/trafficking or general cytotoxicity. For example, HPI-4, a molecule that leads to truncation or loss of the PC,[18] and vinblastine, a drug known to disrupt the assembly of microtubules,[19] both appear as Hh pathway antagonists in a Gli-luciferase reporter assay (Figure 2a

dx.doi.org/10.1021/cb300028a | *ACS Chem. Biol.* 2012, 7, 1040−1048

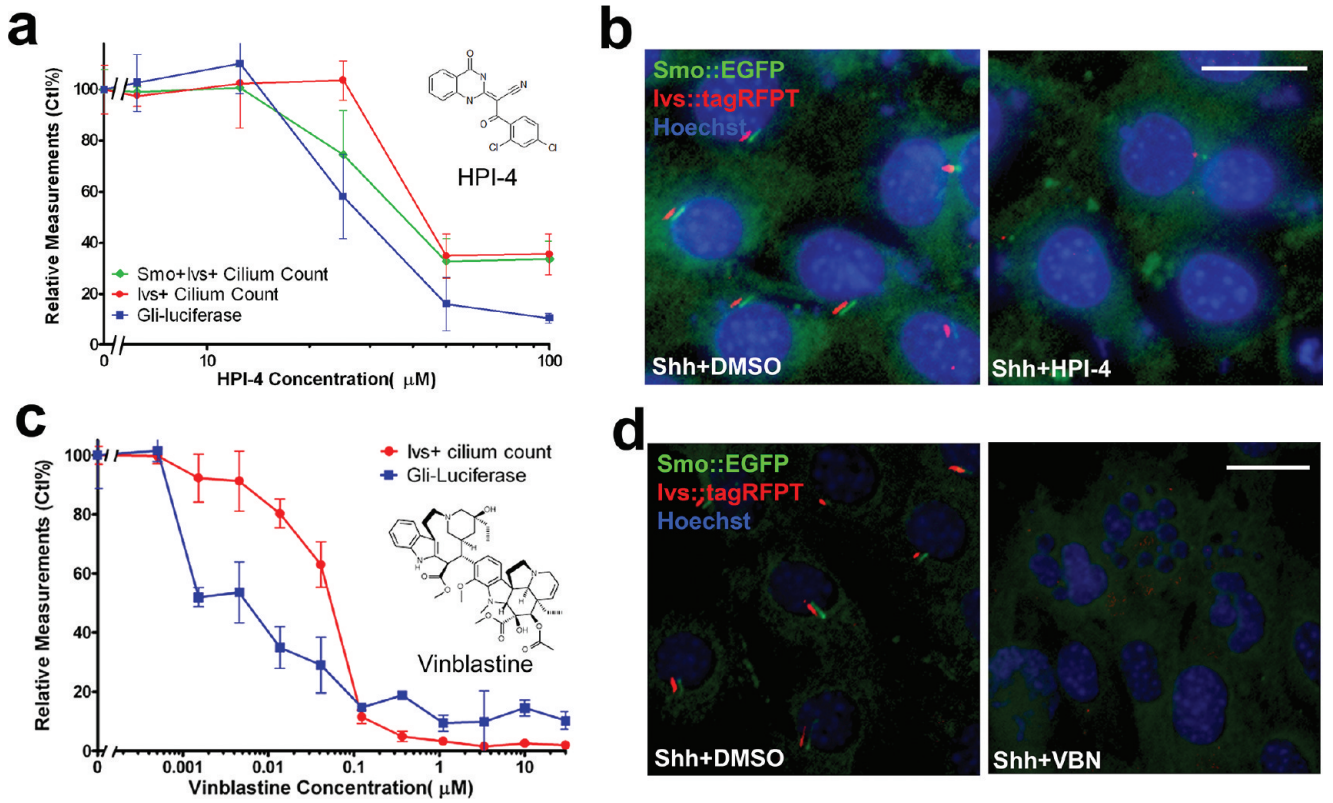

Figure 2. Identification of compounds disrupting the PC. (a,b) HPI-4, an inhibitor of ciliogenesis, was identified in the assay. Please note that throughout this paper Ctrl% is an additional normalization over the mean of DMSO (with or without Shh) treatment as 100%, unless stated otherwise, such as "Ctl = 1". (c,d) Vinblastine (VBN), which disrupts microtubules and leads to disruption of the PC, was also identified through general effects on Ivs::tagRFPT; the mean (±SD) for the Smo localization assay and Gli-luciferase transcriptional reporter assays was calculated from four replicates (panels a and c). HPI-4 and VBN were used at 50 μM and 370 nM, respectively, to generate the representative images in panels b and d. Scale bar: 10 μm.

and c). However, the decrease in the Ivs::tagRFPT ciliary signal in the Smo high-content assay indicates a nonspecific mechanism that alters PC structure (Figure 2).

We identified 26 validated hits that could be divided into 20 classes. These hits include known Hh pathway inhibitors such as AntagVIII, a potent phenyl quinazolinone urea derivative (Supplementary Figure 5).[20] Moreover, identification of AY9944, an inhibitor of cholesterol biosynthesis and esterification,[21] adds additional support to the proposed intersection between cholesterol metabolism and the Hh pathway. Hh ligands are covalently modified by cholesterol, and Hh trafficking has been linked to cholesterol transport processes,[22,23] but *in vitro* studies suggest the response of the target cell is actually suppressed when cholesterol biosynthesis is blocked.[24] Our data suggest a potential link with Smo accumulation within the PC (Supplementary Figure 6). Further, in line with a recent report,[25] our screen identified itraconazole and ketoconazole, two antifungal drugs in current clinical use, as Smo inhibitors in the ciliary-based assay (Supplementary Figure 7). In all cases examined, compounds that blocked Smo translocation to the PC inhibited Gli transcription activity (Supplementary Figures 5−7).

DY131 Inhibits Smo Signaling through a Conventional Mechanism. Of the novel compounds, we first selected DY131, a potent hit, for subsequent analysis. DY131 and its analogue GSK4716 inhibited Shh induced accumulation of Smo::EGFP with IC_{50}'s of 0.8 and 2 μM, respectively (Figure 3a−c, Supplementary Figure 8, Table 1). Both DY131 and GSK4716 inhibit Shh induced activation of a Gli-reporter with somewhat higher IC_{50}'s (2 and 10 μM, respectively) (Figure 3d). The absence of an inhibitory activity in a Wnt pathway reporter assay argues for a specific action of DY131 in suppressing Shh action (Supplementary Figure 9).

DY131 and GSK4716 were previously identified as agonists of the estrogen related receptors (ERR).[26,27] However, other ERR/ER ligands, including tamoxifen citrate, 4-hydroxytamoxifen (4-OHT), diethylstilbestrol, and hexestrol, did not alter the accumulation of Smo on the PC in either the presence or absence of Shh (Supplementary Figure 10), arguing against an ERR-based mode of action for DY131 and GSK4716.

To investigate at what level DY131 functions in the Hh pathway, we compared the drug's dose-dependent performance in inhibiting the activities of wild-type Smo and SmoM2 (also named SMOA1), a constitutively active form of Smo with a tryptophan to leucine mutation in the seventh transmembrane domain.[2] This mutation renders Smo markedly less sensitive (IC_{50}'s for SmoM2 are more than an order of magnitude higher than IC_{50}'s for wild-type Smo) to Cyc, SANT-1, and GDC0449-mediated inhibition[15,16,28] (Supplementary Figures 11 and 12). When overexpressed, both wild-type Smo and SmoM2 constitutively localize to the primary cilium.[9,29] In contrast to its potent inhibition of the ciliary accumulation of wild-type Smo following exposure to Hh ligand (Figure 3c) or overexpression of wild-type Smo (Figure 3e and f), DY131 failed to inhibit ciliary localization of SmoM2 or SmoM2 driven activation of transcriptional reporters of pathway activity, at

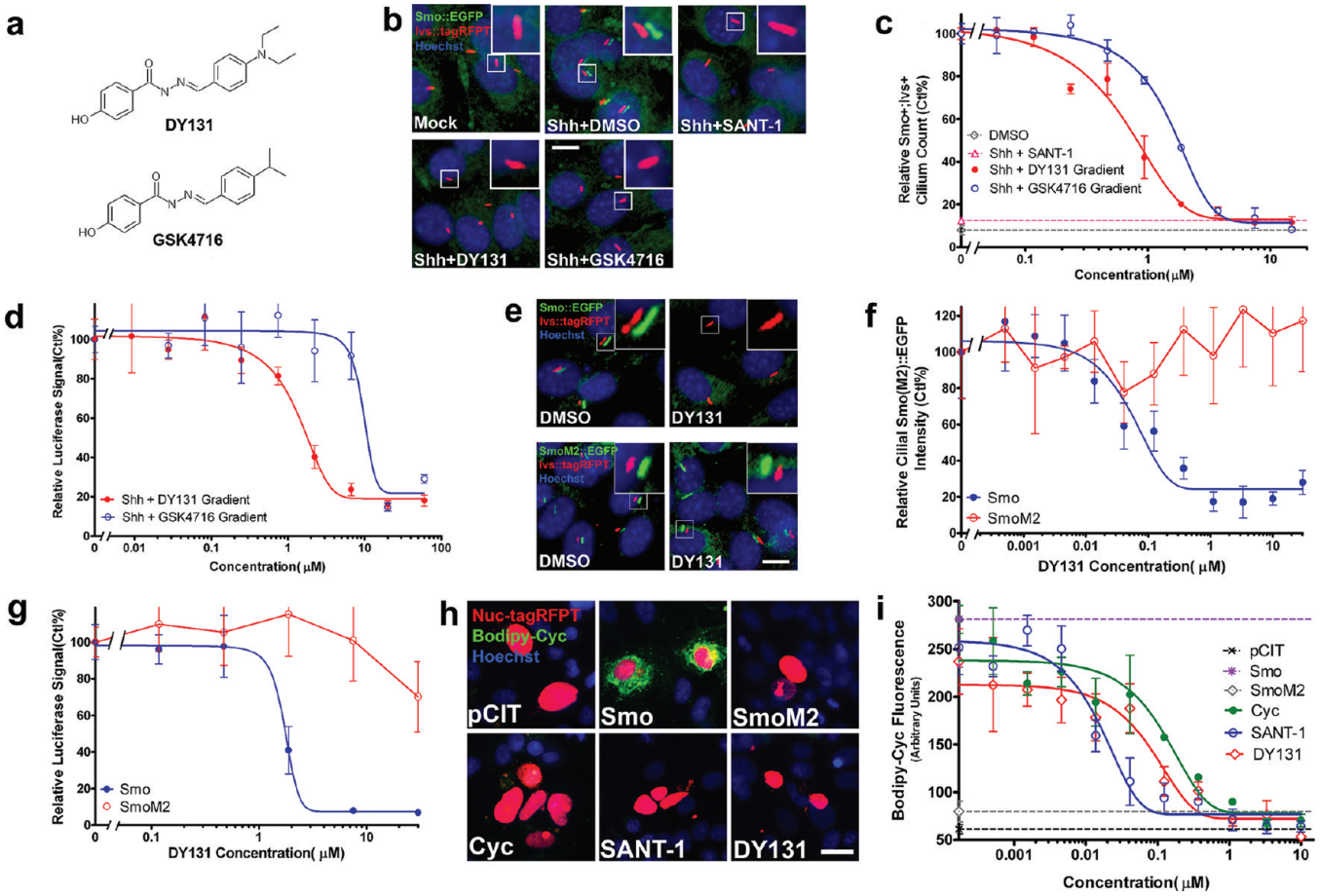

Figure 3. DY131 displays a conserved mechanism for Smo inhibition similar to previously identified antagonists. (a) Structure of DY131 and GSK4716. (b,c) Representative images (b) and quantification (c) of DY131 and GSK4716 inhibition of Hh induced Smo accumulation at the primary cilium; 500 nM SANT-1 was used as a positive control for pronounced inhibition. DY131 and GSK4716 were used at 3.75 and 7.5 μM, respectively, for data in panel b. Scale bar: 5 μm. (d) Gli-luciferase measurements indicate dose-dependent inhibition of Hh pathway activity by both DY131 and GSK4716. Data show the means (±SD) from quadruplicate samples. Image analysis was based on over 300 cells per sample. (e) Representative images showing Smo::EGFP and SmoM2::EGFP overexpressing cells treated with vehicle or 1.1 μM DY131. Scale bar: 5 μm. (f) Image analysis of quadruplicate samples, plotting mean (±SD) of over 300 cells analyzed in each sample. (g) Dose−response curves displaying DY131 inhibition of wild-type Smo and SmoM2 activity. Data show mean (±SD) in quadruplicate samples. Representative images (h) and quantification (i) of Bodipy-Cyc competition experiments. Cyc, SANT-1, and DY131 were each used at 1.1 μM in panel h. Scale bar: 10 μm. Data show the mean (±SD) in quadruplicate samples (i), analyzing 50−100 transfected cells in each sample.

Table 1. IC_{50}'s of Newly Identified Smo Antagonists in Various Cell-Based Assays[a]

cell line	stimulus	measurement	DY131	SMANT
3T3/Smo::GFP/Ivs::tagRFPT	Shh	inhibition of Shh-induced Smo::GFP ciliary accumulation	0.8	1.1
3T3/Shh-LightII	Shh	inhibition of Shh-induced expression of Gli-luciferase reporter	2	2
3T3/Smo::GFP/Ivs::tagRFPT	SAG	inhibition of SAG-induced Smo::GFP ciliary accumulation	2 (100 nM SAG)	>60 (100 nM SAG)
3T3/Shh-LightII	SAG	inhibition of SAG-induced expression of Gli-luciferase reporter	2 (100 nM SAG)	3 (200 nM SAG); 4 (1 μM SAG)
3T3/Smo::GFP Overexpression/Ivs::tagRFPT	none	inhibition of ciliary accumulation of Smo::GFP upon overexpression	0.08	3
3T3/Smo::GFP Overexpression/Shh-LightII	none	inhibition of expression of Gli-luciferase reporter induced by Smo::GFP overexpression	>30	3
3T3/SmoM2::GFP Overexpression/Ivs::tagRFPT	none	inhibition of ciliary localization of SmoM2::GFP	>30	>60
3T3/SmoM2::GFP Overexpression/Shh-LightII	none	inhibition of expression of Gli-luciferase reporter induced by SmoM2::GFP overexpression	>30	1.2
Cos7/Smo expression	none	competition of BODIPY-cyclopamine-Smo binding	0.1	>30
Ptch1± CGNP	Shh	inhibition of Shh induced cell proliferation marked by pH3	<0.625	<0.625

[a]Please note that IC_{50}'s in this paper were obtained through nonlinear regression based on the following equation: Y = bottom + (top − bottom)/(1 + $10^{X-\log IC_{50}}$), where the top and bottom are the Y values of plateaus of no inhibition and saturated inhibition separately.

dx.doi.org/10.1021/cb300028a | ACS Chem. Biol. 2012, 7, 1040−1048

doses up to 30 μM (Figure 3e–g). However, DY131 suppressed SAG (100 nM) induced accumulation of Smo::EGFP in the primary cilium and Gli transcription activity with an IC_{50} of approximately 2 μM (Supplementary Figure 13).

Interestingly, SANT-1 and GDC0449, at a dose high enough to block SmoM2 activity, did not alter SmoM2 ciliary accumulation, suggesting that, as with wild-type Smo, activity of this mutant can be abolished without blocking its localization to the PC (Supplementary Figures 11 and 12).

To determine if DY131 binds directly to Smo, we used a competition assay with bodipy-Cyc, a fluorescent analogue of Cyc.[30] Bodipy-Cyc specifically labels cells overexpressing Smo, co-expressing a red, nuclear fluorescent protein (Nuc-tagRFPT) marker, whereas SmoM2-expressing cells do not bind bodipy-Cyc, confirming the specificity of this assay (Figure 3h and i). DY131, like Cyc and SANT-1, acts as an effective competitor of bodipy-Cyc labeling of cells overexpressing Smo, consistent with either direct binding to Smo at the same site as bodipy-Cyc or at another site on Smo resulting in allosteric modification and loss of bodipy-Cyc binding (Figure 3h and i).

SMANT Inhibits Smo Signaling with a Novel Mechanism. Our data suggest that DY131 and its analogues inhibit Hh signaling through a mechanism similar to that of inhibitors such as Cyc, SANT-1, and GDC0449. However, our focused effort in characterizing most potent hits from the screen also identified small molecules displaying novel behaviors. We named one compound Smo Mutant ANTagonist (SMANT), as it exhibited an equivalent activity in inhibiting SmoM2 and wild-type Smo (Figure 4a and h). SMANT and its analogue SMANT-2 inhibited Shh induced ciliary accumulation of Smo::EGFP with IC_{50}'s of 1.1 and 1.6 μM, respectively (Figure 4b and c; Table 1). Neither resulted in altered Ivs::tagRFPT localization at the PC or profound modulation of Wnt pathway activity, consistent with a Hh pathway-specific mode of action (Figure 4b; Supplementary Figures 14 and 15).

As with DY131, SANT-1, and GDC0449 (Figure 3e and f, Supplementary Figure 11), SMANT failed to block SmoM2::EGFP localization to the PC while potently inhibiting wild-type Smo accumulation (Figure 4d and e). In contrast to some of the other Smo antagonists, SMANT failed to block Smo ciliary localization induced by SAG or Cyc (Figure 4f and g; Supplementary Figure 16; Supplementary Figure 13a and b). However, in contrast to other pathway inhibitors, SMANT was similarly effective at inhibiting Smo and SmoM2 activity and blocked the stimulatory action of SAG at different concentrations in the Gli-luciferase assay (Figures 3d and g and 4h; Supplementary Figure 12 and 13c). SMANT, like DY131 and GDC0449, and distinct from GANT61,[31] a known Gli inhibitor, does not alter Hh pathway activation induced by loss of suFU, a Gli regulatory factor (Figure 4i), suggesting that SMANT functions at the Smo level. However, in contrast with strong competition between DY131 and Cyc for binding Smo (Figure 3h and i), SMANT was a poor competitor (Figure 4j and k), consistent with a unique inhibitory action on Smo activity.

DY131 and SMANT Effectively Inhibit Hh Signaling without the Risk of Rebound Hyperactivity. To further explore the potential utility of compounds found in our assay for developing anticancer agents for Hh pathway targeted therapies, we tested DY131 and SMANT on cultured cerebellar granule neuron precursors (CGNPs) isolated from Ptch1± neonates. Constitutive activation of Hh signaling in these cells

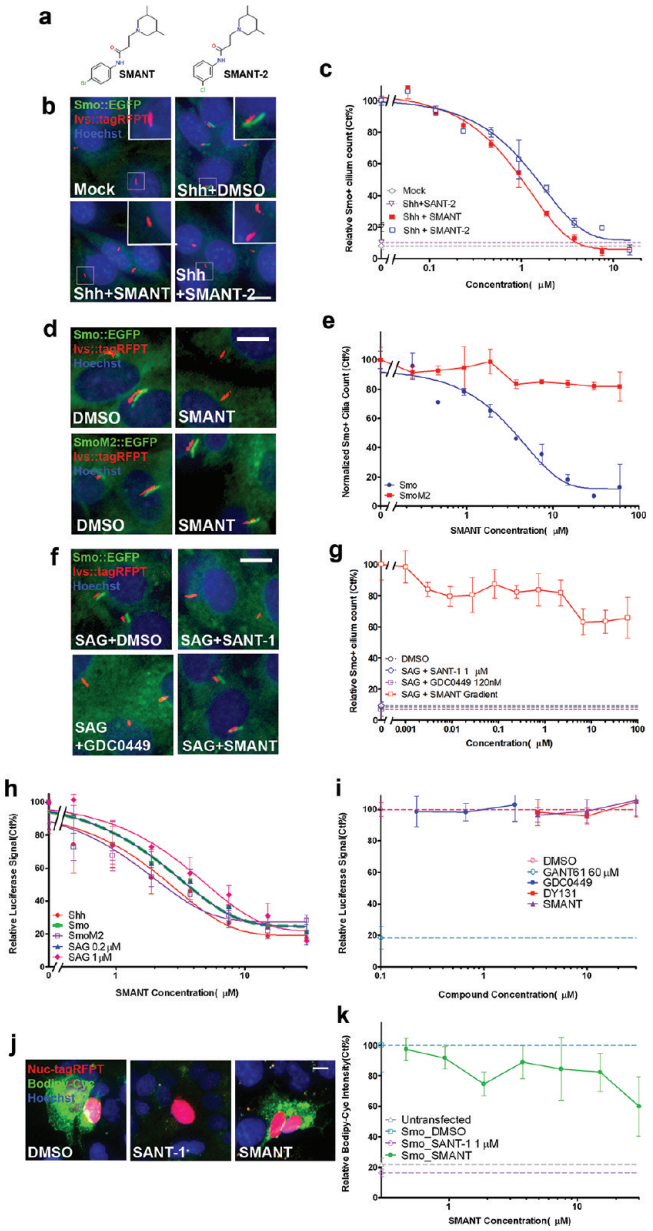

Figure 4. SMANT displays an unprecedented mechanism for Smo inhibition. (a) Structure of SMANT and SMANT-2. (b,c) Representative images (b) and quantification (c) of SMANT and SMANT-2 inhibition of Hh induced Smo accumulation at the primary cilium; 1 μM SANT-2 was used as a positive control. SMANT and SMANT-2 were used at 7.5 μM for data in panel b. Scale bar: 5 μm. (d) Representative images showing Smo::EGFP and SmoM2::EGFP overexpressing cells treated with vehicle or SMANT. SMANT was applied to wild-type Smo and SmoM2 expressing cells at 7.5 and 30 μM, respectively. Scale bar: 5 μm. (e) Image analysis of quadruplicate samples shown in panel d, plotting mean (±SD) of over 300 cells analyzed in each sample. (f,g) Representative images (f) and quantifications of Smo ciliary localization (g) showing Smo::EGFP/Ivs::tagRFPT cells treated with 100 nM SAG combined with vehicle, SANT-1, GDC0449, or SMANT. SANT-1, GDC0449, and SMANT were used at 1 μM, 120 nM, and 60 μM. (h) Gli-luciferase measurement of dose-dependent inhibition of Hh pathway activity by SMANT upon Shh stimulation, overexpression of Smo and SmoM2, respectively, or treatment with 0.2 or 1 μM SAG. Data show the means (±SD) from triplicate samples. (i) Gli-luciferase measurements in suFU−/− mouse embryonic fibroblasts treated with DY131 and SMANT, respectively. GDC0449 and GANT61 were used as

dx.doi.org/10.1021/cb300028a | ACS Chem. Biol. 2012, 7, 1040–1048

Figure 4. continued

negative and positive controls, respectively. (j,k) Representative images (j) and quantification (k) of Bodipy-Cyc competition experiments for SMANT. SANT-1 served as a control for competition activity. SMANT was used at 30 μM in panel h. Scale bar: 5 μm. Data show the mean (±SD) from quadruplicate samples (i), analyzing 100−200 transfected cells in each sample.

is associated with medulloblastoma.[32] Consistent with their potency in inhibiting Hh activity in NIH/3T3 cells, DY131 and SMANT dramatically decreased phosphorylated histone H3 (pH3) marked proliferation of CGNPs induced by Shh (Figure 5a and b).

Finally, we primed cells with GDC0449, Cyc, FKL, or SANT-1 at doses sufficient to decrease both Smo ciliary localization and Gli mediated transcription activity for 24 h (Supplementary Figure 1). Following the removal of drug-containing medium and extensive washing, cells were stimulated with either Hh ligand or the direct-binding Smo agonist SAG.[16,33] As predicted, we observed an elevated signaling response specifically in Cyc and FKL treated cells (Supplementary Figures17a and 18). The hypersensitivity to Hh pathway activation correlated with high levels of Smo that remained within the PC following removal of the antagonizing compound (Supplementary Figure 17b−e). Next we tested the consequences of this effect for newly identified DY131 and SMANT using NIH3T3 cells (Figure 5c) and CGNPs (Figure 5d and e). In contrast to Cyc, we observed no Shh driven hyperactivation of Hh pathway activity on removal of DY131 or SMANT in either the NIH3T3 Gli-luciferase assay or the CGNP proliferation assay.

Discussion. On the basis of evidence presented here, compounds that inhibit both pathway activity and Smo accumulation in the primary cilium have characteristics that may make them reasonably preferred to antagonists that themselves promote ciliary accumulation of Smo. Therefore, the type of high content screen that we have established, which directly quantifies the Smo-PC interactions required for Hh pathway activity, is useful both for discovering new classes of

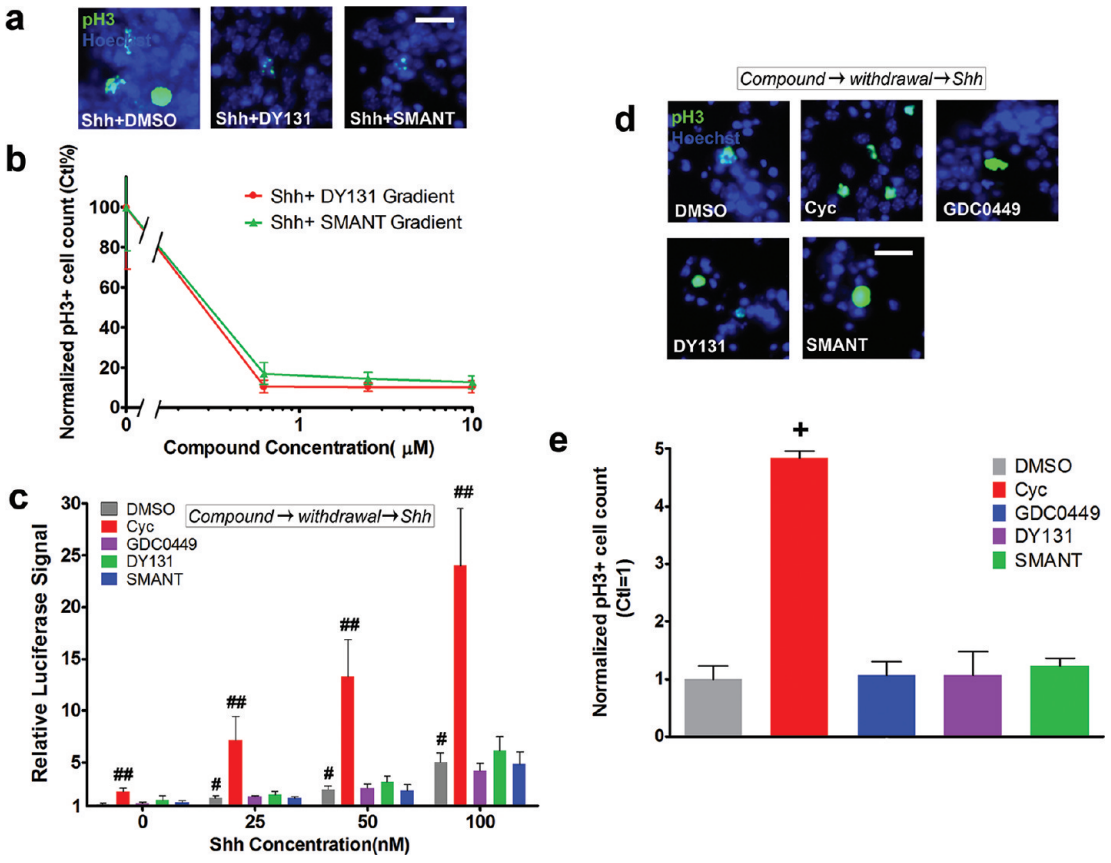

Figure 5. DY131 and SMANT inhibit proliferation of cerebellar granule-cell neural progenitors (CGNP) without conferring hypersensitivity to Shh stimulation. (a,b) Representative images (a) and quantification (b) of phospho-histone H3 (pH3) positive cells upon co-treatment with 0.625 μM DY131 or SMANT with Shh ligand. (b) $P \leq 0.001$ in t test for all samples treated with DY131 or SMANT at 0.625 μM and above compared with DMSO treated controls. (c−e) In contrast to Cyc, GDC0449, DY131, and SMANT do not confer prolonged hypersensitivity to Shh stimulation in either Gli responsive reporter (c) or CGNP proliferation assays (d,e). Hh signaling activity and CGNP proliferation were measured after treatment with vehicle, Cyc (5 μM), GDC0449 (500 nM), DY131 (10 μM), or SMANT (10 μM) separately. Samples were analyzed in quadruplicate; data show the mean (±SD). For the Gli-luciferase reporter assay (c), cells stimulated by Shh for a relatively short time period (12 h) displayed a modest but significant inductive response ($^{\#}p < 0.003$ in a t test comparing to a DMSO primed 0 nM Shh treatment). The response was enhanced by pretreating cells with Cyc ($^{\#\#}P < 0.003$ in t test comparing to DMSO priming and stimulation with the same concentration of Shh), whereas pretreatment with GDC0449, DY131, or SMANT showed no enhancing activity ($P > 0.05$ in t test comparing samples primed with DMSO and stimulated with the same concentration of Shh). For the CGNP assay (d,e), cells were treated for 3 days. $^{+}p < 0.0001$ in a t test comparing the effects of DMSO (control) or any of the antagonists of Smo ciliary accumulation.

dx.doi.org/10.1021/cb300028a | ACS Chem. Biol. 2012, 7, 1040−1048

antagonists and for studying existing ones.The current screen, of over 5,000 compounds, selectively identified a substantial number of small molecules with efficacy in this assay and more conventional Hh pathway assays. While careful analysis of DY131 suggests a direct interaction with Smo, SMANT shows a unique profile inhibiting an oncogenic form of Smo carrying the M2 mutation with efficacy similar to that of its wild-type counterpart. The differing properties of SMANT when compared with a variety of other Smo modulators (SAG, Cyc, GDC0449, and SANT-1) are consistent with a SMANT inhibitory action at a site on Smo different to that bound by these other compounds or an indirect modulation of Smo activity. Smo can be inactivated in the PC by SMANT when harboring the M2 mutation or after SAG driven translocation to the PC, suggesting that SMANT may inactivate both the oncogenic form and an SAG-bound form of Smo, and more importantly, the ciliary localization of Smo and its activation may be mechanistically divergent. It is possible that post-translational modifications, conformation changes, or interacting partners that regulate ciliary entry or accumulation of Smo differ from those governing activity in the primary cilium.[34,35] Frequently, compounds show a higher potency in the inhibition of Smo localization to the primary cilium compared to that in Gli-luciferase assays (Figure 3c and d, Figure 4 c and h, Supplementary Figures 5−7). This could reflect pathway activity while Smo is out of the PC or the different time frames involved in the two assay systems.

Our studies highlight new opportunities for therapeutic development that may potentiate existing approaches and offer new strategies toward treatment of resistant forms of Smo emerging from somatic mutation. The screening platform provides a robust assay system. The Smo ciliary screen broadly interrogates a key aspect of HH pathway regulation and biology and potentially identifies small molecule regulators that may not score in a conventional transcriptional end-point assay. These compounds may nevertheless provide a reasonable grounding for subsequent drug development. Further, the screen enables a stratification of small molecule function in the HH pathway and a platform that can be extended to potentially explore ciliopathies, an increasingly important area of medical significance.[36]

METHODS

Cell Culture. NIH/3T3 cells were maintained in DMEM containing 10% (v/v) calf serum, penicillin, streptomycin, and L-glutamine. HEK293, L, cos7, and suFU−/− mouse embryonic fibroblast cells were maintained in DMEM containing 10% (v/v) fetal bovine serum, penicillin, streptomycin, and L-glutamine. Smo::EGFP, SmoM2::EGFP, and Ivs::tagRFPT were cloned into pBabe to generate retroviral particles for infection. Smo::EGFP/Ivs::tagRFPT and SmoM2::EGFP/Ivs::tagRFPT stable cell lines were generated through viral infection of NIH/3T3.[13] A ShhLightII Gli reporter cell line was obtained from the American Type Culture Collection (ATCC) and used in luciferase reporter assays to measure Hh pathway activity. The cell line contains a stably integrated Gli-responsive Firefly luciferase reporter and a constitutive *Renilla* luciferase expression construct.[28] Subclones expressing Smo or SmoM2 in ShhLightII cells were used for chemical epistasis analyses.

Shh conditioned medium, which is collected from cos7 cells transfected with an expression construct encoding the amino terminal 19 kDa signaling peptide of Shh, was used at 13.7 ± 3.0 nM. Wnt3a conditioned medium was collected from an L-cell line producing Wnt3a ligand.[37] Controls utilized supernatants from cos7 cells transfected with empty vector or a wild-type L-cell line.

Reagents. Cyclopamine and forskolin were purchased from Sigma. SAG, SANT-1, GDC0449, and BODIPY-cyclopamine were purchased from Axxora Platform, Tocris Biosciences, Selleck Chemicals, and Toronto Research Chemicals, respectively. All small molecule stock solutions were prepared by dissolving in DMSO at 10 mM and stored at −20 °C. Mouse recombinant ShhN purified protein (IIShhN) was purchased from R&D Systems.

Transfection was performed using Fugene6 or Fugene HD from Roche.

Imaging Assays. Cells were cultured and treated in 384-well imaging plate precoated with poly-D-lysine (Greiner Bio-one), fixed with 4% (w/v) paraformaldehyde (Electron Microscopy Sciences), and stained with Hoechst (Invitrogen). Images were collected using Opera High Content Screening System (Perkin-Elmer). ActivityBase (IDBS Inc.,) and Pipeline Pilot (Accelrys, Inc.) were used for high content screening data management and analysis.

Image Analysis of Smo Ciliary Localization. Acapella 2.0 software (Evotec Technologies/PerkinElmer) was used to perform multiparametric high content image quantification. Our image analysis script used Ivs::tagRFPT to first determine the location of the PC and then Smo::EGFP to quantify the level of Smo present in the cilium.

First, we used the spot-finding algorithm in the RFP channel to find Ivs-rich spots. Each nonoverlapping spot was based on a maximum 8-pixel radius (when using a 40x objective) around a central intensity peak of 5 pixels. A distance of at least 10 pixels was required between adjacent spot centers. Spot peaks had to exceed thresholds of relative intensity compared to the remaining body of the spot as well as to the entire image. The average, maximum, and total RFP intensities of each spot were measured. The spots with sufficiently high absolute maxima to pass the selected threshold were classified as positive spots. To form candidate cilia, we selected the brightest 15% of the pixels in each positive spot and merged those pixels into objects so that the brightest parts of adjacent spots could form single, larger cilia-shaped objects. To qualify the candidate cilia as true Ivs-positive cilia, the width of the objects created from merging the brightest pixels in each spot had to be at least 2 pixels and the length to half-width ratio had to exceed 3 (*i.e.*, a 3-pixel long by 2-pixel wide cilium was the minimum accepted cilium size and the length had to be at least 1.5-fold the width). The mean GFP intensity within these Ivs-positive cilia was used to estimate the ciliary level of Smo protein. We found it necessary to subtract the background of the mean GFP intensity in the 3-pixel wide area around each candidate cilium to avoid some false positives. Those Ivs-positive cilia that exceed the final mean GFP intensity threshold set for each experiment were deemed Smo-positive cilia.

Hoechst staining was used to determine the total number of nuclei per well.

The final output measurements of the number of Ivs-positive cilia in the well, the number of Smo-positive cilia in the well, and the mean GFP intensity of the accepted cilia within the well were used to calculate if a compound qualified as an inhibitor and to estimate the quality of inhibition. Inhibitors of smoothened accumulation into the cilia were initially chosen as compounds that had numbers of Ivs-positive cilia per nucleus (or per field of view) similar to the DMSO controls but fewer Smo-positive cilia compared to the DMSO controls. Compounds that generated many fewer Ivs-positive cilia were judged as either defective in cilium assembly/trafficking or generally toxic depending on the morphology of the cells. Measurements of the geometry of the cilia as well as the total fluorescent intensities of each cilium in the Smo and Ivs channels were used to determine if any of the compounds were having unusual effects on cilia size, intensity, or frequency of observation or combinations of all three characteristics.

The thresholds and parameters used in selecting, classifying, and quantitating spots, candidate cilia, and nuclei were applied uniformly for every well in each set of plates prepared as a single batch with the same set of cells and reagents. We used diagnostic images during threshold selection to outline which objects (spots, candidate cilia, candidate nuclei, etc.) passed or failed each selection. At least 2 fields of positive controls (Shh + SANT-1) and negative controls (Shh + DMSO) were examined for threshold setting. Visual observation and Z-prime calculations measuring the ability of the assay to distinguish

positive from negative controls were used for quality control on each batch of plates and set of thresholds. All images for comparison were scanned with identical microscopic settings and analyzed with the same input parameters.

Hh and Wnt Activity Assays. Hh activity assays were performed using ShhLightII cells, Smo/LightII cells, SmoM2/LightII cells, and suFU−/− mouse embryonic fibroblasts. In the suFU−/− cells, Hh activity was measured after co-transfection with Gli driven firefly luciferase and TK-renilla luciferase reporters.[38] Wnt activity was measured in 293 cells co-transfected with Top-flash and TK-renilla luciferase reporters.[39] Cells were cultured and treated in 96-well assay plates (Corning) and incubated with Duo-Glo luciferase substrates-(Promega) to measure firefly and renilla luciferase activity sequentially using a TopCount NX Microplate Scintillation and Luminescence Counter (Perkin-Elmer). The renilla luciferase signal was used to normalize the firefly reporter activity.

Bodipy-Cyclopamine Competition Assays. Cos7 cells were transfected with a plasmid co-expressing *Smo* and a nuclear localized form of tagRFPT (pCIT-Smo). An empty parental construct (pCIT), and a construct that co-expresses *SmoM2* were used as controls to assess specificity and background noise. Three days after transfection, cells were incubated with 5 nM Bodipy-cyclopamine, with or without other compounds, for 1 h at 37 °C. Cells were washed, fixed, and stained with Hoechst. Images were collected by an Opera High Content Screen System. Bodipy fluorescence was quantified specifically for transfected cells (determined by red tagRFPT+ nucleus) using a program developed by the authors with Acapella 2.0 software. All of the images were scanned with identical microscopic settings and analyzed with the same input parameters.

CGNP Proliferation Assays. CGNP primary cells were isolated from P7 *Ptch1*± mice as previously reported[40] and immediately seeded in poly-D-lysine coated imaging plates (Greiner Bio-one). Compounds were applied 2 h post seeding, for either 36 (Figure 5a and b) or 72 h (Figure 5d and e). After completion of each experimental regimen, cells were fixed with 4% paraformaldehyde (Electron Microscopy Sciences) and stained with anti-pH3 antibody (Upstate; 1:100) followed by a secondary antibody (Invitrogen) and Hoechst (Invitrogen). Images were then collected using a confocal microscope. Cell proliferation, as marked by a pH3 signal, was quantified with an in-house program developed by the authors using Acapella 2.0 software. Identical microscopic settings were used in each analysis, and identical input parameters were implemented for each experiment.

■ ASSOCIATED CONTENT

Ⓢ Supporting Information

This material is available free of charge *via* the Internet at http://pubs.acs.org.

■ AUTHOR INFORMATION

Corresponding Author

*E-mail: amcmahon@mcb.harvard.edu; lee_rubin@harvard.edu.

Present Addresses

[¶]The Morgridge Institute for Research, Madison, WI 53715.
[#]The Scripps Research Institute, La Jolla, CA 92037.
[□]Blue Sky Biotech, Inc., Worcester, MA 01605.
[▽]Dartmouth Medical School, Hanover, NH 03755.

Notes

The authors declare the following competing financial interest(s):Y.W., L.L.R., and A.P.M. hold patent positions around Hedgehog signaling and drug discovery platforms.

■ ACKNOWLEDGMENTS

We are very grateful to C. T. Walsh, S. L. Schreiber, A. Saghatelian, and T. Curran for critical review of our results and helpful discussions. We thank J. W. Lichtman, R. Y. Tsien, M. P. Scott, and P. T. Chuang for sharing reagents. We thank R. A. Segal and X. Zhao for technical assistance on CNGP cell culture and our colleagues in the McMahon and Rubin laboratories for support of our research. We are also grateful to R. Hellmiss at Harvard Center of Biological Imaging for help with artwork. This work was supported by a grant from Harvard Stem Cell Institute (DP-0033-08-02 to A.P.M and L.L.R) and a grant from National Institutes of Health (R37 NS033642 to A.P.M.).

■ REFERENCES

(1) McMahon, A. P., Ingham, P. W., and Tabin, C. J. (2003) Developmental roles and clinical significance of hedgehog signaling. *Curr. Top. Dev. Biol. 53*, 1−114.

(2) Xie, J., Murone, M., Luoh, S. M., Ryan, A., Gu, Q., Zhang, C., Bonifas, J. M., Lam, C. W., Hynes, M., Goddard, A., Rosenthal, A., Epstein, E. H., Jr., and de Sauvage, F. J. (1998) Activating Smoothened mutations in sporadic basal-cell carcinoma. *Nature 391*, 90−92.

(3) Romer, J. T., Kimura, H., Magdaleno, S., Sasai, K., Fuller, C., Baines, H., Connelly, M., Stewart, C. F., Gould, S., Rubin, L. L., and Curran, T. (2004) Suppression of the Shh pathway using a small molecule inhibitor eliminates medulloblastoma in Ptc1(±)p53(−/−) mice. *Cancer Cell 6*, 229−240.

(4) Yauch, R. L., Gould, S. E., Scales, S. J., Tang, T., Tian, H., Ahn, C. P., Marshall, D., Fu, L., Januario, T., Kallop, D., Nannini-Pepe, M., Kotkow, K., Marsters, J. C., Rubin, L. L., and de Sauvage, F. J. (2008) A paracrine requirement for hedgehog signalling in cancer. *Nature 455*, 406−410.

(5) Rubin, L. L., and de Sauvage, F. J. (2006) Targeting the Hedgehog pathway in cancer. *Nat. Rev. Drug Discovery 5*, 1026−1033.

(6) Scales, S., and de Sauvage, F. (2009) Mechanisms of Hedgehog pathway activation in cancer and implications for therapy. *Trends Pharmacol. Sci. 6*, 303−312.

(7) Von Hoff, D., Lorusso, P., Rudin, C., Reddy, J., Yauch, R., Tibes, R., Weiss, G., Borad, M., Hann, C., Brahmer, J., Mackey, H., Lum, B., Darbonne, W., Marsters, J., de Sauvage, F., and Low, J. (2009) Inhibition of the hedgehog pathway in advanced basal-cell carcinoma. *N. Engl. J. Med. 361*, 1164−1172.

(8) Allison, M. (2012) Hedgehog hopes lifted by approval... and stung by failure. *Nat. Biotechnol. 30*, 203.

(9) Corbit, K. C., Aanstad, P., Singla, V., Norman, A. R., Stainier, D. Y. R., and Reiter, J. F. (2005) Vertebrate Smoothened functions at the primary cilium. *Nature 437*, 1018−1021.

(10) Rohatgi, R., Milenkovic, L., and Scott, M. P. (2007) Patched1 regulates hedgehog signaling at the primary cilium. *Science 317*, 372−376.

(11) Wilson, C. W., Chen, M.-H., and Chuang, P.-T. (2009) Smoothened adopts multiple active and inactive conformations capable of trafficking to the primary cilium. *PLoS One 4*, e5182.

(12) Rohatgi, R., Milenkovic, L., Corcoran, R., and Scott, M. (2009) Hedgehog signal transduction by Smoothened: Pharmacologic evidence for a 2-step activation process. *Proc. Natl. Acad. Sci. U.S.A. 106*, 3196−3201.

(13) Wang, Y., Zhou, Z., Walsh, C., and McMahon, A. (2009) Selective translocation of intracellular Smoothened to the primary cilium in response to Hedgehog pathway modulation. *Proc. Natl. Acad. Sci. U.S.A. 106*, 2623−2628.

(14) Dijkgraaf, G. J., Alicke, B., Weinmann, L., Januario, T., West, K., Modrusan, Z., Burdick, D., Goldsmith, R., Robarge, K., Sutherlin, D., Scales, S. J., Gould, S. E., Yauch, R. L., and de Sauvage, F. J. (2011) Small molecule inhibition of GDC-0449 refractory smoothened mutants and downstream mechanisms of drug resistance. *Cancer Res. 71*, 435−444.

(15) Yauch, R., Dijkgraaf, G., Alicke, B., Januario, T., Ahn, C., Holcomb, T., Pujara, K., Stinson, J., Callahan, C., Tang, T., Bazan, J., Kan, Z., Seshagiri, S., Hann, C., Gould, S., Low, J., Rudin, C., and de Sauvage, F. (2009) Smoothened mutation confers resistance to a

hedgehog pathway inhibitor in medulloblastoma. *Science 326*, 572–574.
(16) Chen, J. K., Taipale, J., Young, K. E., Maiti, T., and Beachy, P. A. (2002) Small molecule modulation of Smoothened activity. *Proc. Natl. Acad. Sci. U.S.A. 99*, 14071–14076.
(17) Zhang, J. H., Chung, T. D. Y., and Oldenburg, K. R. (1999) A simple statistical parameter for use in evaluation and validation of high throughput screening assays. *J. Biomol. Screening 4*, 67–73.
(18) Hyman, J., Firestone, A., Heine, V., Zhao, Y., Ocasio, C., Han, K., Sun, M., Rack, P., Sinha, S., Wu, J., Solow-Cordero, D., Jiang, J., Rowitch, D., and Chen, J. (2009) Small-molecule inhibitors reveal multiple strategies for Hedgehog pathway blockade. *Proc. Natl. Acad. Sci. U.S.A. 106*, 14132–14137.
(19) Jordan, M. A., and Wilson, L. (2004) Microtubules as a target for anticancer drugs. *Nat. Rev. Cancer 4*, 253–265.
(20) Brunton, S. A., Stibbard, J. H. A., Rubin, L. L., Kruse, L. I., Guicherit, O. M., Boyd, E. A., and Price, S. (2008) Potent inhibitors of the hedgehog signaling pathway. *J. Med. Chem. 51*, 1108–1110.
(21) Incardona, J. P., and Eaton, S. (2000) Cholesterol in signal transduction. *Curr. Opin. Cell Biol. 12*, 193–203.
(22) Lewis, P. M., Dunn, M. P., McMahon, J. A., Logan, M., Martin, J. F., St-Jacques, B., and McMahon, A. P. (2001) Cholesterol modification of sonic hedgehog is required for long-range signaling activity and effective modulation of signaling by Ptc1. *Cell 105*, 599–612.
(23) Li, Y. N., Zhang, H. M., Litingtung, Y., and Chiang, C. (2006) Cholesterol modification restricts the spread of Shh gradient in the limb bud. *Proc. Natl. Acad. Sci. U.S.A. 103*, 6548–6553.
(24) Cooper, M. K., Wassif, C. A., Krakowiak, P. A., Taipale, J., Gong, R., Kelley, R. I., Porter, F. D., and Beachy, P. A. (2003) A defective response to Hedgehog signaling in disorders of cholesterol biosynthesis. *Nat. Genet. 33*, 508–513 ; correction vol 34, p 113.
(25) Kim, J., Tang, J. Y., Gong, R., Lee, J. J., Clemons, K. V., Chong, C. R., Chang, K. S., Fereshteh, M., Gardner, D., Reya, T., Liu, J. O., Epstein, E. H., Stevens, D. A., and Beachy, P. A. (2010) Itraconazole, a commonly used antifungal that inhibits Hedgehog pathway activity and cancer growth. *Cancer Cell 17*, 388–399.
(26) Yu, D. D., and Forman, B. M. (2005) Identification of an agonist ligand for estrogen-related receptors ERRbeta/gamma. *Bioorg. Med. Chem. Lett. 15*, 1311–1313.
(27) Zuercher, W. J., Gaillard, S., Orband-Miller, L. A., Chao, E. Y., Shearer, B. G., Jones, D. G., Miller, A. B., Collins, J. L., McDonnell, D. P., and Willson, T. M. (2005) Identification and structure-activity relationship of phenolic acyl hydrazones as selective agonists for the estrogen-related orphan nuclear receptors ERRbeta and ERRgamma. *J. Med. Chem. 48*, 3107–3109.
(28) Taipale, J., Chen, J. K., Cooper, M. K., Wang, B., Mann, R. K., Milenkovic, L., Scott, M. P., and Beachy, P. A. (2000) Effects of oncogenic mutations in Smoothened and Patched can be reversed by cyclopamine. *Nature 406*, 1005–1009.
(29) Han, Y.-G., Spassky, N., Romaguera-Ros, M., Garcia-Verdugo, J.-M., Aguilar, A., Schneider-Maunoury, S., and Alvarez-Buylla, A. (2008) Hedgehog signaling and primary cilia are required for the formation of adult neural stem cells. *Nat. Neurosci. 11*, 277–284.
(30) Chen, J. K., Taipale, J., Cooper, M. K., and Beachy, P. A. (2002) Inhibition of Hedgehog signaling by direct binding of cyclopamine to Smoothened. *Genes Dev. 16*, 2743–2748.
(31) Lauth, M., Bergström, A., Shimokawa, T., and Toftgård, R. (2007) Inhibition of GLI-mediated transcription and tumor cell growth by small-molecule antagonists. *Proc. Natl. Acad. Sci. U.S.A. 104*, 8455–8460.
(32) Schuller, U., Heine, V. M., Mao, J., Kho, A. T., Dillon, A. K., Han, Y. G., Huillard, E., Sun, T., Ligon, A. H., Qian, Y., Ma, Q., Alvarez-Buylla, A., McMahon, A. P., Rowitch, D. H., and Ligon, K. L. (2008) Acquisition of granule neuron precursor identity is a critical determinant of progenitor cell competence to form Shh-induced medulloblastoma. *Cancer Cell 14*, 123–134.
(33) Frank-Kamenetsky, M., Zhang, X. M., Bottega, S., Guicherit, O., Wichterle, H., Dudek, H., Bumcrot, D., Wang, F. Y., Jones, S., Shulok, J., Rubin, L. L., and Porter, J. A. (2002) Small-molecule modulators of Hedgehog signaling: identification and characterization of Smoothened agonists and antagonists. *J. Biol. 1*, 10.
(34) Chen, Y., Sasai, N., Ma, G., Yue, T., Jia, J., Briscoe, J., and Jiang, J. (2011) Sonic Hedgehog dependent phosphorylation by CK1alpha and GRK2 is required for ciliary accumulation and activation of smoothened. *PLoS Biol. 9*, e1001083.
(35) Su, Y., Ospina, J. K., Zhang, J., Michelson, A. P., Schoen, A. M., and Zhu, A. J. (2011) Sequential phosphorylation of smoothened transduces graded hedgehog signaling. *Sci. Signaling 4*, ra43.
(36) Nigg, E. A., and Raff, J. W. (2009) Centrioles, centrosomes, and cilia in health and disease. *Cell 139*, 663–678.
(37) Willert, K., Brown, J. D., Danenberg, E., Duncan, A. W., Weissman, I. L., Reya, T., Yates, J. R., 3rd, and Nusse, R. (2003) Wnt proteins are lipid-modified and can act as stem cell growth factors. *Nature 423*, 448–452.
(38) Nybakken, K., Vokes, S. A., Lin, T. Y., McMahon, A. P., and Perrimon, N. (2005) A genome-wide RNA interference screen in Drosophila melanogaster cells for new components of the Hh signaling pathway. *Nat. Genet. 37*, 1323–1332.
(39) Corbit, K. C., Shyer, A. E., Dowdle, W. E., Gaulden, J., Singla, V., and Reiter, J. F. (2008) Kif3a constrains beta-catenin-dependent Wnt signalling through dual ciliary and non-ciliary mechanisms. *Nat. Cell Biol. 10*, 70–76.
(40) Chan, J. A., Balasubramanian, S., Witt, R. M., Nazemi, K. J., Choi, Y., Pazyra-Murphy, M. F., Walsh, C. O., Thompson, M., and Segal, R. A. (2009) Proteoglycan interactions with Sonic Hedgehog specify mitogenic responses. *Nat. Neurosci. 12*, 409–417.